View metadata, citation and similar papers at core.ac.uk

brought to you by CORE

provided by Elsevier - Publisher Connector

Available online at www.sciencedirect.com

ScienceDirect

Energy Procedia 57 (2014) 1908– 1921

Energy Procedia

2013 ISES Solar World Congress

THERMAL BEHAVIOR OF GREEN ROOF IN REUNION ISLAND: CONTRIBUTION TOWARDS A NET ZERO BUILDING

MORAU Dominique[a]* , RAKOTONDRAMIARANA Hery Tiana[b], RANAIVOARISOA Tojo Fanomezana[b], ANDRIAMAMONJY Ando Ludovic[b]

[a]Laboratory PIMENT, University of La Reunion 117 Rue du Général Ailleret 97430 Le Tampon REUNION (FRANCE), [b]Institute for the Management of Energy (IME), University of Antananarivo, PoBox 566 Antananarivo 101 (Madagascar)

Abstract

A green roof is an option for improving a building thermal comfort. The investigation is here performed within the specific climate context of Reunion Island in south hemisphere. This type of roof system involves choice difficulties for plant species that are more favorable to establish that comfort.

The objective of this work is to simulate the dynamic behavior of this system towards external requests in wet tropical zones and vis-à-vis influences of certain number of physical parameters related to this system.

As long as possible, authors used the electrical analogy method to establish a mathematical model associated to the studied system. Based on this model, a Matlab computing code was finalized. Weather data of Reunion Island were used for simulations; the green roof potential and benefit were highlighted by surveying the temperature gain and the heat flux crossing the roof as well as the energy saving performance. Furthermore, the energy consumption being surveyed while doing sensitivity analysis with Fourier Amplitude Sensitivity Test method, the most influential parameters of the model were identified.

Full scale experimental results are provided and consisting in monitoring green roof on the top of a public building. According to the results, we can assert that the green roof decreases heat flux entering through the roof during the day and restrains the restoration of accumulated heat at night. Indeed, the support on which the plantation ground bases affects the building thermal insulation.

The experimental data are also conducted to prove the effectiveness of thermal insulation by green roofs in reducing temperature in the building between 5°C and 7°C in relation to plants type and the canopy Leaf Area Index (LAI).

A comparison of experimental values and model results is done. Among other uses, this code can be used as a tool for choosing the plants and the drain materials to be experimented on the green roof. The results offer hints to optimize the design and thermal performance of extensive green roofs.

© 2014 The Authors. Published by Elsevier Ltd. This is an open access article under the CC BY-NC-ND license (http://creativecommons.org/licenses/by-nc-nd/3.0/).

Selection and/or peer-review under responsibility of ISES.

***Keywords*: Green roof, thermal comfort, building, modeling, computing code, sensitivity analysis, wet tropical zone, solar energy.**

* Corresponding author. Tel.: + 262 57 91 41; fax: + 262 57 94 46.
E-mail address: dominique.morau@univ-reunion.fr

1876-6102 © 2014 The Authors. Published by Elsevier Ltd. This is an open access article under the CC BY-NC-ND license (http://creativecommons.org/licenses/by-nc-nd/3.0/).
Selection and/or peer-review under responsibility of ISES.
doi:10.1016/j.egypro.2014.10.055

1. Introduction

Green roofs are considered to be an effective solution to improve internal and external environment at the building and urban levels. In comparison to conventional roofs, green roofs improve storm water management [1, 2], reduce air pollution [3, 4] and noise [5]. Green roofs increase vegetal and animal biodiversity in cities [6, 7] and they also reduce a city's carbon footprint by converting carbon dioxide to oxygen through photosynthesis [4, 8]. Green roofs improve the thermal insulation of a building. Thereby reducing solar heat gain by approximately 70-90% in the summer and reducing heat loss by approximately 10-30% in the winter [9].

Two types of green roofs are generally identified: extensive (with soil thickness less than 10-15 cm) and intensive (with soil thickness more than 15-20 cm) [2, 8]. Extensive green roofs are suitable for building retrofitting and they do not require any additional strengthening [10]. The choice of green roofs characteristics depends on the weather conditions and plant species [11].

The number of studies regarding this problematic are developed as ROOFSOL research project [12], which focused on the theoretical and experimental analysis of different roof solutions for cooling in the Mediterranean region, mainly based on evaporative and radiative cooling principles. In the case of Greece, the work of Niachou et al. [13] as well as the study of Spala et al. [14] on the analysis of the green roof thermal properties and energy performance can be considered.

The green roof technology is also able to reduce the energy consumption and to improve the internal comfort during the spring and summer seasons, in sites where the climatology is characterized by high temperature and irradiance values during the day [15].

There is a growing literature data regarding the green roof energy balance. An important work has been performed by both experimental and computational methods [16, 17, 18].

Few studies were investigated in the Southern hemisphere where the green roof potential as a natural cooling is unknown or poorly known. Wong et al. [19, 20] explored the thermal benefits of a green roof in Singapore through an experimental test done before and after the construction of a rooftop garden. A comparison between climates plants, substrate, etc, between Australia and European countries was realised by William NSG [21].

In this study, a comprehensive analysis of the impacts of green roofs on the thermal performance of building is presented, including experimental study and modelling. To validate the model experimentally, the numerical results are compared with experimental data. Furthermore, the energy consumption being surveyed while doing sensitivity analysis with Fourier Amplitude Sensitivity Test method, the most influential parameters of the model were identified.

2. Green roof model

2.1. A bibliographic review of green roof models

In the literature, many green roof models are available ranging from simple to detailed. The simplest model considers only the decrease of the roof U-value [13, 22]. Other studies have presented more details models, with a heat balance that considers additional influencing phenomena such as solar shading by foliage and cooling by evapotranspiration [23, 24, 25, 26].

Table 1 realised by Djedjig [27] summarizes various existing green roofs models [10, 24], which differ in their approaches. The proposed model in this paper considers the soil mass transfer in which precipitation, watering and drainage are taken into account in addition to vapor exchange in order to assess the effect of humidity transfer on thermal exchange. Besides, heat transfer through drain layer is separated from that taking place in the soil as presented in § II.2.

Table 1. A bibliographic review of green roof models.

Model	Assumptions	Description
(E.Barrio, 1998) [23]	Renewable thermal air zone within the foliage	The model is solved for a constant temperature and the water content of the soil
(D.J. Sailor and S.Frankenstein and G.Koenig, 2004) [24,28]	Negligible thermal inertia of the substrate and constant proportions of the air mixture within the foliage	The model is based on two balances equations for the foliage and soil surface
(E. Alexandri and P. Jones, 2007) [29]	Non – uniformity of the temperature and humidity fields throughout the foliage canopy	An overall heat balance throughout the extensive roof
(C. Feng et al.,2010) [8]	Photosynthesis is significant and the leaf temperature is known	Solving a reduced form of the partial differential equations of transfer
(H.He and C.Y.Jim, 2010) [30]	A multilayer foliage canopy with semitransparent radiative properties	Development of an efficiency shading model (SEM) based on the theory of propagation of electromagnetic waves
(S-E. Ouldboukhitine, 2011) [31]	Negligible thermal inertia of the substrate and constant proportions of the air mixture within the foliage	Based on a modified version of Sailor's model that accounts for the effect of water transfer on the thermal properties of substrate using Penman -Monteith
(P.C.tabares-Velasco, 2011) [32]	Steady-state regime and negligible thermal inertia of the substrate	Model based on experimental observations of a setup

2.2. Presentation of the proposed model

Generally, as illustrated on Figure (1.a), the green roof is composed of: a vegetation layer known as canopy, a soil layer, a drainage layer and the waterproof concrete support. The coverage ratio σ_f and the LAI (Leaf Area Index) characterize the canopy. These parameters respectively vary according to seasons and the canopy plant type. In what follows, we mean by "ordinary roof", the roof made by only the concrete support as indicated on Figure (1.b). To show the interest of the green roof, from the energy performance point of view, compared to the ordinary roof, we will compare the energy saving performances of both roof types.

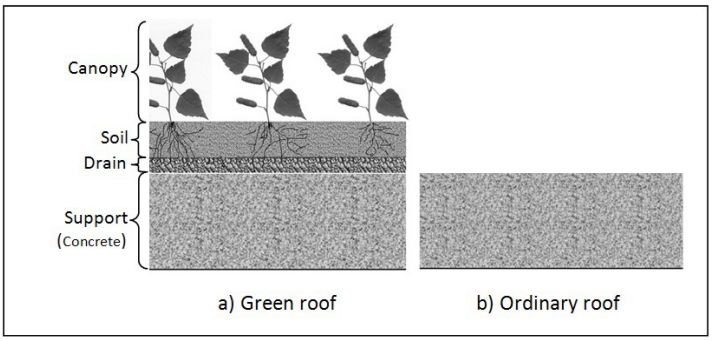

Fig. 1: Sketch of both surveyed roof types

2. 2.1. Simplifying hypotheses for the green roof modelling

The following assumptions are adopted [33]: the problem is monodimensional; the temperatures of canopy foliage and canopy air are considered as uniform respectively; the water contents of soil substrate and drainage layers are time dependent but constant in space; ground and canopy layers are mulch free. Canopy plants are healthy and at the stage of growth. Heat transfer by conduction through plants is negligible. Plants, soil and drain layers are supposed horizontally homogeneous.

2. 2.2. Thermal and mass balance equations of the green roof

Thermal and mass balance equations of the green roof can be written per ground area unit as follows:

- **Thermal balance**
  - At the canopy foliage node:

$$d_f.LAI.\left(\rho c_p\right)_a \frac{\partial T_p}{\partial t} = \sigma_f \Big[(1-\tau_s-(1-\tau_s)\rho_\infty)\left(1+\tau_s\rho_g\right)\varphi_s + \varepsilon_g\sigma\left(T_{sky}^4 - T_p^4\right) + \frac{\varepsilon_g\varepsilon_p\sigma}{\varepsilon_g+\varepsilon_p+\varepsilon_g\varepsilon_p}\left(T_{gt}^4 - Tp4+2LAI\rho cpare\ Ta-Tp+2LAI\rho cpa\gamma rs+re\ ea-ep\right. \quad (1)$$

  - On the canopy air node:

$$L_c\left(\rho c_p\right)_a \frac{\partial T_a}{\partial t} = 2.LAI.\frac{\left(\rho c_p\right)_a}{r_e}\left(T_p - T_a\right) + h_g\left(T_{gt} - T_a\right) + \tau_e L_c\left(\rho c_p\right)_a\left(T_m - T_a\right) + 2.LAI.\frac{\left(\rho c_p\right)_a}{\gamma(r_s+r_e)}\left(e_p - e_a\right) + \frac{\left(\rho c_p\right)_a}{\gamma r_e}\left(e_g - e_a\right) \quad (2)$$

  - On the soil nodes:

$$\begin{cases} \left(\rho c_p\right)_g \frac{\partial T_g}{\partial t} = \frac{\partial}{\partial z}\left[\lambda_g \frac{\partial T_g(z,t)}{\partial z}\right] \\ -\lambda_g \frac{\partial T_g(z,t)}{\partial z}\Big|_{z=0} = \left(1-\rho_g\right)\left(1-\sigma_f(1-\tau_s)\rho_\infty\right) + \frac{\varepsilon_g\varepsilon_p\sigma\sigma_f}{\varepsilon_g+\varepsilon_p+\varepsilon_g\varepsilon_p}\left(T_p^4 - T_{gt}^4\right) + \\ \left(1-\sigma_f\right)\sigma\left(T_{sky}^4 - T_{gt}^4\right) + h_g\left(T_a - T_{gt}\right) - \frac{h_g}{\gamma}\left(e_p - e_a\right) \end{cases} \quad (3)$$

  - On the drain nodes:

$$\begin{cases} \left(\rho c_p\right)_d \frac{\partial T_d(z,t)}{\partial t} = \frac{\partial}{\partial z}\left[\lambda_d \frac{\partial T_g(z,t)}{\partial z}\right] \\ -\lambda_d \frac{\partial T_d(z,t)}{\partial z}\Big|_{z=0} = -\lambda_g \frac{\partial T_g(z,t)}{\partial z}\Big|_{z=L_g} \end{cases} \quad (4)$$

  - On the support nodes:

$$\begin{cases} \left(\rho c_p\right)_s \frac{\partial T_s(z,t)}{\partial t} = \lambda_s \frac{\partial^2 T_s(z,t)}{\partial z^2} \\ -\lambda_d \frac{\partial T_d(z,t)}{\partial z}\Big|_{z=L_g} = -\lambda_s \frac{\partial T_s(z,t)}{\partial z}\Big|_{z=0} \\ -\lambda_s \frac{\partial T_s(z,t)}{\partial z}\Big|_{z=L_s} = h_{in}(T_{sb} - T_{in}) \end{cases} \quad (5)$$

- **Mass balance**
  - On the canopy air node:

$$L_c\rho_a\frac{\partial\theta_a}{\partial t}=\frac{h_g}{\gamma.\Lambda(T_{gt})}\left(e_g-e_a\right)+\frac{1}{\gamma.\Lambda(T_a)}\tau_e L_c\left(\rho c_p\right)_a\left(e_m-e_a\right)+2.LAI.\frac{\left(\rho c_p\right)_a}{\gamma.\Lambda(T_p).(r_s-r_e)}\left(e_g-e_a\right) \quad (6)$$

  - On the soil node:

$$\rho_w L_g\frac{\partial w_g(t)}{\partial t}=P_{re}+A_r+D_r-\left[-\frac{h_g}{\gamma.\Lambda(T_{gt})}\left(e_g-e_a\right)-2.LAI.\frac{\left(\rho c_p\right)_a}{\gamma.\Lambda(T_p).(r_s+r_e)}\left(e_p-e_a\right)\right] \quad (7)$$

where, for the following nomenclatures, subscripts $a, g, in, m, p, s, d,$ and sky respectively denote the following green roof system subcomponents: canopy air, green roof soil (gt for its top face), indoor air, outdoor ambient air, canopy leaves, support (sb for its bottom face and st for its top face), drain (dt for its top face), and sky vault.

Hence, in equations (1) to (7), T_i is the temperature of subcomponent i (K), $\left(\rho c_p\right)_i$ is the specific heat capacity of subcomponent i $(J.m^{-2}.K^{-1})$, ρ_a is canopy air density $(kg.m^{-3})$, LAI is the canopy Leaf Area Index ( ), σ_f is the canopy foliage coverage ratio (%), σ is Stefan-Boltzmann constant $(W.K^{-1})$, d_f is the average leaves thickness (m), L_i is the thickness of subcomponent i (m), ε_i is the emissivity of subcomponent i ( ), ρ_g is the ground reflectance ( ), ρ_∞ is the reflectance of a dense canopy ( ), φ_s is solar shortwave irradiance at the top of the canopy $(W.m^{-2})$, $\Lambda(T_i)$ is the latent heat of vaporization at the temperature T_i $(J.kg^{-1})$, h_{in} is thermal convective coefficient between the support bottom and the indoor air $(W.m^{-2}.K^{-1})$ and its model is given by reference [34], h_g is thermal convective coefficient between the soil top face and the canopy air $(W.m^{-2}.K^{-1})$ and its model is proposed in reference [35], σ_s is the canopy shortwave transmittance ( ), τ_e is ratio of air exchange, (e_i-e_a) is the partial vapor pressure deficit (Pa) between the subcomponent i $(i=p,g)$ and the canopy air, γ is the thermodynamic psychrometric constant $(Pa.K^{-1})$, P_{re} is the precipitation $(kg.m^{-2}.s^{-1})$, A_r is the watering $(kg.m^{-2}.s^{-1})$, D_r is the drainage $(kg.m^{-2}.s^{-1})$, λ_i is the thermal conductivity of the subcomponent i $(i=p,g,s)$ $(W.m^{-1}.K^{-1})$ and λ_g being particularly given by reference [29], w_g is the soil volumetric moisture content ( ), r_e is the canopy external resistance $(s.m^{-1})$, r_s is the bulk stomatal resistance $(s.m^{-1})$; models of resistances r_e et r_s proposed by reference [23] were adopted for this investigation.

2. 2.3. Thermal balance equations of the ordinary roof

$$\begin{cases}\left(\rho c_p\right)_s\frac{\partial T_s^*(z,t)}{\partial t}=\lambda_s\frac{\partial^2 T_s^*(z,t)}{\partial z^2}\\ -\lambda_s\frac{\partial T_s^*(z,t)}{\partial z}\Big|_{z=0}=\varepsilon_{st}\varphi_S-\varepsilon_{st}\sigma\left(T_{st}^{*4}-T_{sky}^4\right)-h_{out}(T_{st}^*-T_m)\\ -\lambda_s\frac{\partial T_s^*(z,t)}{\partial z}\Big|_{z=L_s}=h_{in}(T_{sb}-T_{in})\end{cases} \quad (8)$$

where, nomenclatures given for equations (1) to (7) being still available, T_{st}^* and T_{sb}^* are the nude support top and bottom faces temperatures respectively whereas ε_{st} is its emissivity and h_{out} is the thermal convective coefficient between the support top face and the outdoor air $(W.m^{-2}.K^{-1})$, given by reference [36].

3. Experiment

The experimental green roof was established on August-September 2010 and is still in progress. The green roof is located in the South of Reunion Island, in Saint-Pierre town (21°19' S, 55°28' E) which is in an area under the wind and at 55 m above the sea level. There is a tropical humid climate along the coast and rather temperate in the mid – highlands.
A reference bituminous roof is located nearby this experimental green roof (Figure 2). Both the reference roof and the green roof have no slope and the same area (54 m^2). The green roof is also characterized by a maximal weight of 170 kg/m^2 and a water retention capacity reaching 40 L/m^2.

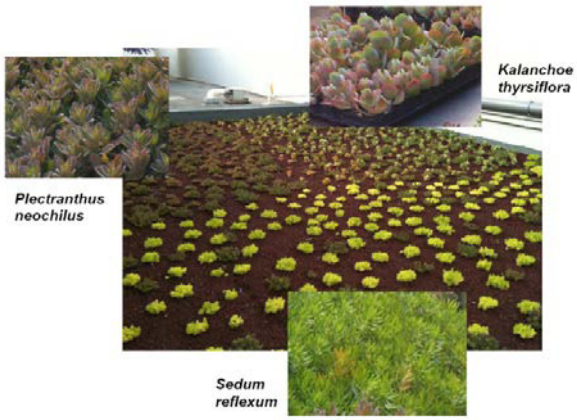

Fig. 2: Plants constituting the green roof

4. Method

4.1. Numerical resolution

For developing a Matlab computing code to survey the system thermal behavior, the proposed model equations are linearized and discretized by steps of time and space, using the finite differences method. Then, the obtained system of linear equations is solved by matrix method, for each step of time, and by successive iterations until convergence.

4.2. Energy performance assessment

The energy consumption per area unit for both cooling and heating was evaluated. It is directly related to the quantity of heat flux entering or leaving through the roof support and which can be written as follows:

$$\varphi = \frac{1}{R_{th}}(T_{st} - T_{in}) \quad (9)$$

with

$$R_{th} = \frac{L_s}{\lambda_s} + \frac{1}{h_{in}} \quad (10)$$

where, nomenclature given for equations (1) to (8) being still available, φ is the heat flux entering or outgoing through an unit area of the roof support ($W.m^{-2}$) and R_{th} is the bulk thermal resistance of the roof support ($K.m^2.W^{-1}$).

To investigate the energy performance of both roof types, we followed the same method as proposed by Sébastien [37]. Indeed, a positive value of heat flux φ represents an entry of heat through the roof (thus a need for cooling) while a negative value of heat flux represents a loss of heat through the roof (thus a need for heating).

To present the demand for energy necessary to mitigate the heat flux crossing the roof, we assume that a system of cooling and heating with a 100% yield will consume, to ensure a constant indoor air temperature, the same number of kilowatt-hour that the energy which entered or left the building through the roof and for the same period of times. So for a given day, for example, if it was entered 2 (kWh) through the support, we would assume that 2 (kWh) were spent by the cooling system to keep constant the indoor air temperature. Similarly, if 1.2 (kWh) were lost through the roof for the same day, we assume that 1.2 (kWh) were spent by the heating system to preserve a constant indoor air temperature.

Thereafter, the instant heat flux being calculated for each time step, the daily number of kilowatt-hour entering and outgoing per area unit through the supports of both roof types can be computed by integrating the heat flux versus time curve; in other words, calculating the surface bounded by the above mentioned curve and the time-axis. As heat fluxes are calculated with sufficiently small time step, the sum of kilowatt-hour obtained over 24 hours can be obtained by means of rectangular method, that is, the sum over 24 hours of the product of the instant flux value (kW) and the time step (h). Then, the difference between consumption energy quantities respectively related to the ordinary roof and the green roof represents the saved energy.

5. Results and discussions

As most of the temperature and heat flux values were normally distributed, parametric statistics were applied. Data were expressed as means ± standard deviation values. The level of significance of $\alpha = 0.05$ was accepted in all cases.

5.1 Effect of the green roof on temperature fluctuations

During the experimental period, the maximum ambient air temperature was 28.7±0.4°C and the maximum temperature of the reference roof reached 73.5±1.4°C. The presence of plants significantly decreased the temperature of the roof surface (between the RR surface and the GR Surface) whatever their species. Indeed, results obtained over the experimental five-month period showed that the maximum temperature measured under the three species of plants reached an average of 34.8±0.6°C (table 2). Accordingly, Wong et al. [19] reported that the maximum temperature measured under different kinds of vegetation in Singapore, which is also influenced by a tropical environment but under an equatorial climate, was closed to 36.0°C.

Table 2. Temperature difference between GR Surface and GR at 120 mm (°C)

MONTH	PLECTRANTHUS	KALANCHOE	SEDUM
Oct.	9.2 ± 2.1	8.0 ± 1.3	8.0 ± 2.5
Nov.	11.2 ± 0.5	9.0 ± 2.0	6.8 ± 0.6
Dec.	5.7 ± 0.5	4.6 ± 1.1	6.2 ± 0.9
Jan.	3.6 ± 1.0	4.8 ± 0.6	6.1 ± 0.6
Feb.	4.6 ± 0.2	5.9 ± 0.2	6.3 ± 0.5

5.2 Effect of the green roof on heat flux variations

Figure 3A illustrates the global solar radiation values and the comparison of heat flux transferred through the different green roof components according to the plant species (Figure 3B) on three typical days in January. Whereas the mean value of maximum global solar radiation on three days was 1165.7±43.3 W/m^2, the maximum heat flux transferred through *Plectranthus* green roof surface was 27.7±2.2 W/m^2, leading to determine a transmitted heat flux exchange of 2.4±0.2%. With *Kalanchoe*, the maximum heat flux reached a mean value of 28.8±2.7 W/m^2 that corresponded to a 2.5±0.3% of transmitted heat flux. For *Sedum*, it appeared a mean value of heat flux at 16.6±1.7 W/m^2, resulting into a heat flux exchange of 1.4±0.2% and suggesting that energy performance of *Sedum* is better than those of *Plectranthus* and *Kalanchoe*.

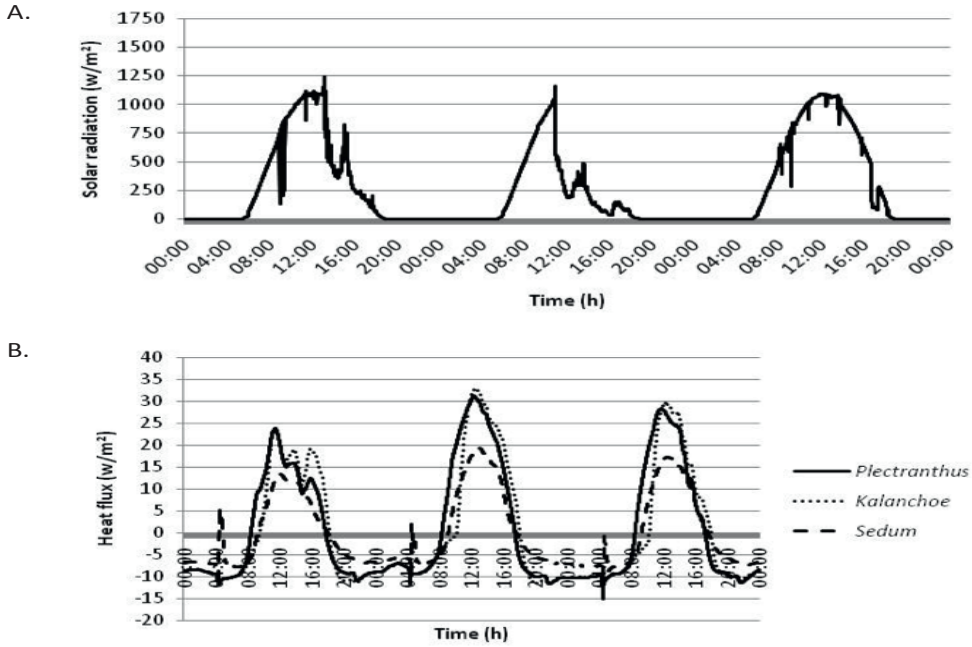

Fig. 3: Effect of the green roof on heat flux variations in January 2011.
Global solar radiations (A) and heat fluxes (B) were measured on three typical days

During all the experimental five-month period, our study also shows that *Sedum* green roof presented an average heat flux exchange of 1.4±0.3% as compared to *Plectranthus* (2.3±0.2%) and *Kalanchoe* (2.2±0.4%) green roofs. This result agrees with the data published by Feng et al. [8] establishing a heat flux exchange of 1.2% for *Sedum* green roof. Here, the higher performance of *Sedum* could be related to its higher sun-shading effect as well as its higher ability to grow more quickly than *Plectranthus* and *Kalanchoe*. For Wong et al. [19], the thermal protection of plants also highly depends on their leaf area index (LAI) since lower temperatures were found under dense trees and shrubs as compared to sparse foliages.

As the green roof energy performance depends on its ability to reduce the heat gain, we measured the heat gain/loss per square meter over the five-month period. Considering that the total solar radiation did not significantly change during this period (1215.9±32.0 W/m^2), it could be observed that the presence of the green roof was associated with an average total heat gain decreasing over the time. Indeed, from

October to February, the total heat gain decreased from 1095.6±158.7–760.4±42.0 kJ/m^2 for the green roof with *Plectranthus*. For *Kalanchoe* green roof, the total heat gain reduced from 858.0±90.4–657.3±58.8 kJ/m^2. With *Sedum* green roof, the total heat gain also significantly decreased from 795.6±174.9–443.6±99.7 kJ/m^2. Such a decrease in the total heat gain value observed with the green roof can be explained by the growth of plants offering a higher coverage and a better roof membrane protection. Our data demonstrated that the green roof with *Sedum* led to a higher restitution of heat gain (63%) than the green roof with *Plectranthus* (54%) and *Kalanchoe* (51%).

5.3 Sensitivity analysis outcome

A sensitivity analysis of the proposed green roof model was carried out by means of FAST method (Fourier Amplitude Sensitivity Test) [36]. Energy consumption being the surveyed model output, Figures (4) and (5) respectively present the decreasing order of dominance of the most influential parameters of the model for diurnal and night periods.

In Figures (4) and (5), nomenclatures given for equations (1) to (7) being still available, az_s denotes the solar azimuth angle (rd), h_s is the solar elevation angle (rd), rho_g represents the soil top face reflectance ( ), R_{dirh} and R_{difh} are beam and diffuse solar radiations respectively $(W.m^{-2})$, hr denotes the outdoor air relative humidity (%), eps_g is the ground top face emissivity ( ), τ_t is the canopy foliage shortwave radiation transmittance ( ), w_{ds} represents the drain volumetric moisture content at saturation $(kg.kg^{-1})$, u is wind speed $(m.s^{-1})$, w_{gs} is the substrate volumetric moisture content at saturation $(kg.kg^{-1})$, $inclin$ and az_t respectively denotes the inclination and azimuth angles of the green roof (rd).

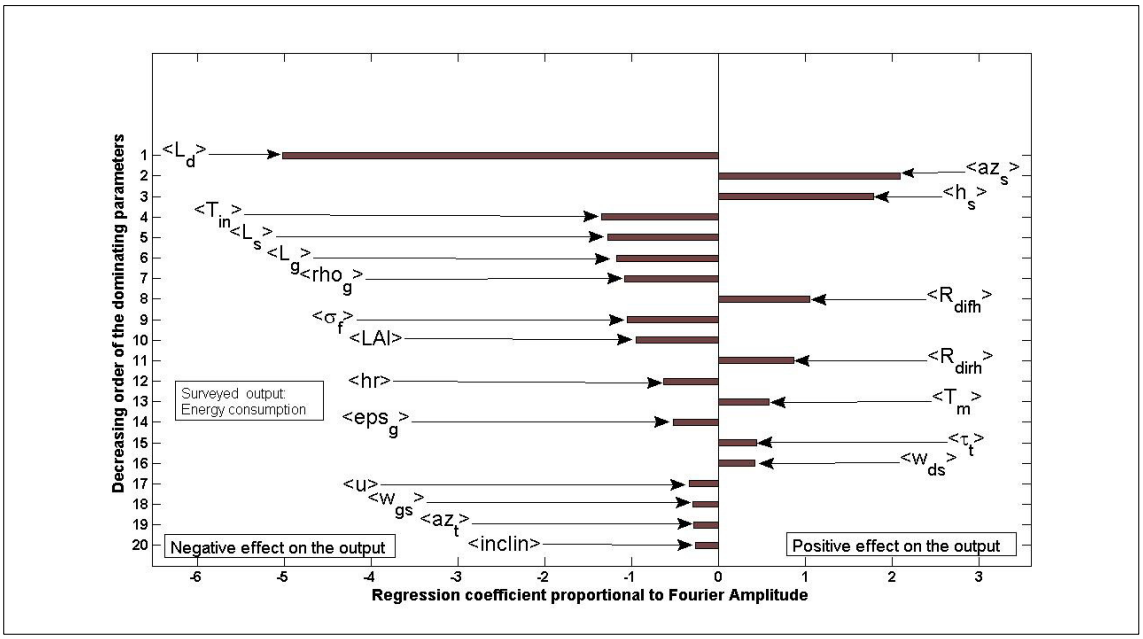

Fig.4: Comparison of the influential parameters of the proposed model during diurnal period

According to Figures (4) and (5), the drain layer thickness L_d is the most dominating parameter of the model during both diurnal and night periods, and has a negative effect on the energy consumption. The high magnitude of model sensitivity vis-à-vis this factor is likely due to the drain mass transfer sub-model that was adopted in this investigation. However, the negative effect of this factor on the energy consumption is coherent as it has the same sense of influence as other green roof subcomponent layer

thicknesses. Indeed, support and ground layer thicknesses (L_s and L_g) have also negative effects on the energy consumption. As high values of the soil, the drain and the support layer thicknesses would reduce the energy consumption, in the one hand, and can entail an excess of weight that can whether alter the structure of the support or increase the building construction costs, in the other hand, it would be interesting to carry out a technical-economical optimization of the values of the three aforementioned factors.

For both diurnal and night periods, the desired indoor air temperature value T_{in} is significantly influential on the model output and has negative effect on the energy consumption while its values range from 15 (°C) to 26 (°C).

In diurnal period (see Figure (4)), weather forcing factors such as: solar azimuth angle az_s, solar elevation angle h_s, beam and diffuse solar radiations (R_{dirh} and R_{difh}) as well as the outdoor air temperature T_m, are influential and have positive effects on the energy consumption. Among these factors, the two first ones are the most influential, which means, the raise of energy consumption is dependent on the Sun position, in other words, on the day time naturally. In the contrary, relative humidity hr and wind speed u have negative effects on the energy consumption but their influences are less significant than the four first other abovementioned weather forcing factors. Moreover, in order to reduce energy consumption, the soil top face should have high values of reflectance rho_g and emissivity eps_g; otherwise, the canopy foliage coverage ratio σ_f and LAI values should be high at least. Besides, the drain volumetric moisture content at saturation w_{ds} and the substrate volumetric moisture content at saturation w_{gs} behave towards the output model differently. While the first, that is more influential, has positive effect on energy consumption, the latter has negative effect on it. At last, orientation az_t and slope of the green roof $inclin$ can be helpful to reduce energy consumption even though their negative effects are the least significant ones.

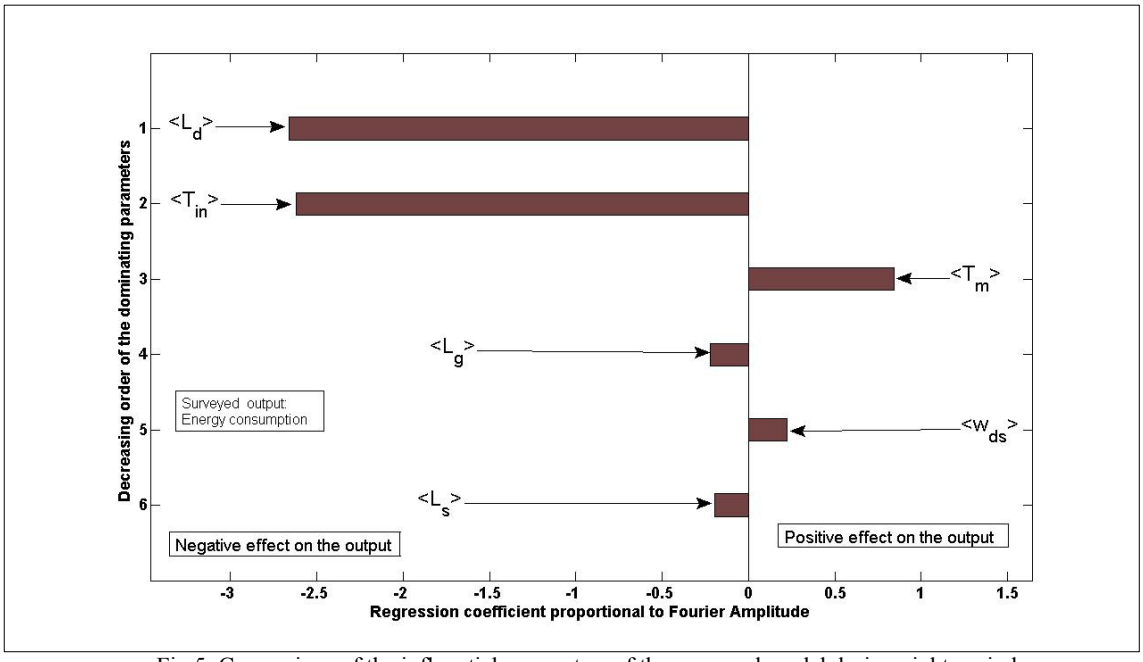

Fig.5: Comparison of the influential parameters of the proposed model during night-period

In night period (Figure 5), only six factors matter and their senses of effect on the energy consumption remain the same as those obtained in the diurnal period, namely: the drain, ground and support layer

thicknesses ($L_d, L_g,$ and L_s), the indoor and outdoor air temperatures (T_{in} and T_m) as well as the drain volumetric moisture content at saturation w_{ds}.

The model sensitivity analysis outcome justifies our choice of separating heat and mass transfer balance equation from that of soil.

5.4. Comparison of simulation and experimental results

January 2011 weather data of Réunion island, were used for simulations. The time and space steps are respectively equal to 30 (s) and 5 (mm).

For the green roof performance survey, the indoor air temperature was varied between values ranging from 15 (°C) to 26 (°C). In the other simulations, the indoor air temperature is fixed at 20 (°C).

Besides, the following properties values were adopted:

For the canopy: LAI=3, $\rho_f = 80\%$, $k_1 = 0.8$ (longwave radiation extinction coefficient), $\rho_\infty = 0.2$, $\tau_l = 0.2$, $L_c = 0.1(m)$, $d_f = 0.001(m)$.

The canopy was assumed to evaporate more than a tomato crop (f =1.1 > 1)

For the soil: apparent density$\rho_d = 1250$ $(kg/m^3$, volumetric water content at saturation $w_{gs} = 40$ (%), $L_g = 0.08\ (m)$,

For the drain:L_d *=0.04 (m),* $\rho_d = 1150$ (kg/m^3). For the green roof and the conventional roof, the support was assumed to be made of the same concrete with *Ls = 0.2 (m)*

Figure 6 shows the variation curves of the temperature difference observed at the top face support of both roof types respectively obtained from simulation and experimental measurement. The two curves adopt an identical look. However, the temperature difference ΔT is positive, that is, the temperature of the ordinary roof top face support is higher than that of the green roof, from 8:30 am to 3:30 pm for the experimental curve whereas this positive temperature gain occurs from 10:00 am to 5:30 pm for the simulation curve. Elsewhere, the temperature difference ΔT is negative. Accordingly, we can assert that the green roof decreases heat flux entering through the roof during the day and restrains the restoration of accumulated heat at night. Indeed, the support on which the plantation ground bases affects the building thermal insulation.

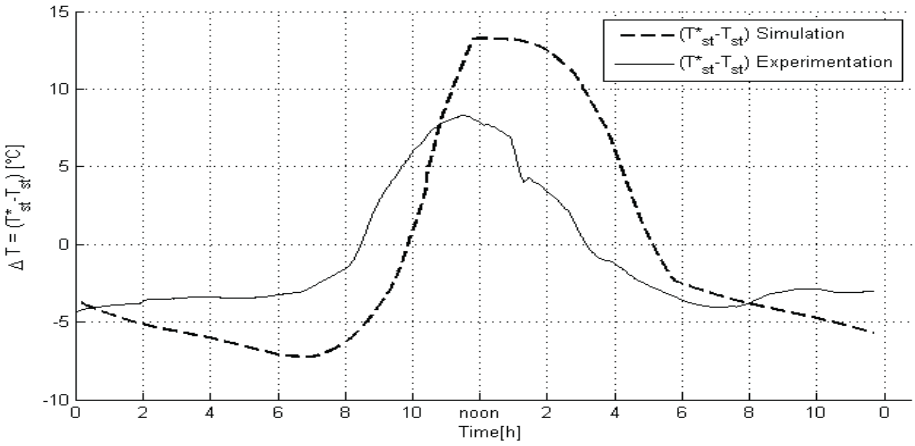

Fig.6: Comparison of temperature difference ($\Delta T = T^*_{st} - T_{st}$) curves respectively obtained from simulation and experimentation

For diurnal period, figure 7 shows that the higher is LAI value, the lesser is the heat flux crossing the green roof. Accordingly, energy consumption related to cooling, that is represented by symbol C on figure (7) legend (while symbol H for heating), is lesser when LAI value is higher. Then, this canopy characteristic parameter influences the green roof refreshing power in diurnal period.

Figure 8 presents a comparison of energy performances of both considered roof types. It shows that for keeping the indoor air temperature value between 15 (°C) and 26 (°C), the ordinary roof requires more cooling/heating energy consumption than the green roof does. Furthermore, energy saving is maximum when the indoor air temperature value is in the standard thermal comfort range, that is, between 20 (°C) and 24 (°C).

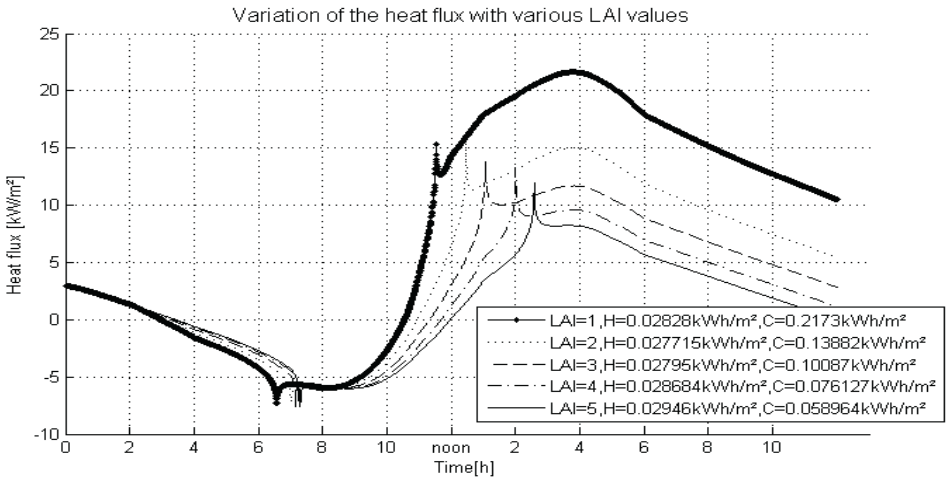

Fig.7 : Influence of the parameter LAI on the heat flux

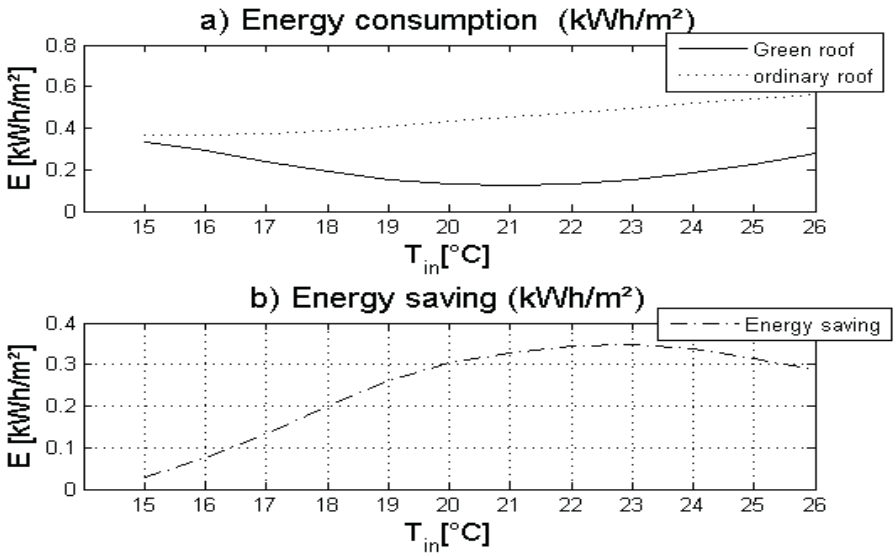

Fig.8: Comparison of energy performances of ordinary and green roofs

The green roofs consistently reduced the average daily heat flow through the roof throughout the year more in summer (70 – 80 %) and less in the winter (20 – 30 %). This again confirmed that extensive green roofs could improve the energy efficiency of the roofing system, particularly effectively in reducing heat gain in the summer.

6. Conclusion

This study aimed to evaluate for the first time the thermal and energy performance of an extensive green roof in an Indian Ocean area under a tropical humid climate. Our results showed that the green roof induced a significant decrease in temperature fluctuations between the green roof surface and the green roof at the depth of 120 mm (6.7±0.1°C). Each plant also contributed to a low heat flux exchange through the green roof. *Sedum* presented an average heat flux exchange of 1.4±0.3% as compared to *Plectranthus* (2.3±0.2%) and *Kalanchoe* (2.2±0.4%). As the energy performance of a green roof mainly depends on its ability to reduce the heat gain, we compared the values of heat gain/loss per meter square over all the five months of experimentation. It was found that *Sedum* green roof led to a higher heat restitution rate with 63%, than for *Plectranthus* (54%) and *Kalanchoe* (51%).

It ensues from simulation results confronted with experimental ones obtained in the Laboratory PIMENT of the University of La Reunion, that the temperature gains are positive in diurnal period and negative in night-period. Green roof can so favour energy saving in building thermal comfort process.

The model sensitivity analysis outcome justifies our choice of separating heat and mass transfer balance equation from that of soil.

The impact of the LAI parameter on energy consumption is not proportional. In order for green roofs to have a significant impact on energy demand, an optimal LAI level should be found with consideration of interacting parameters, such the foliage density.

To conclude, this study has evaluated for the first time the thermal and energetic performance of a green roof in an Indian Ocean area. Our results contribute to highlight *Sedum* benefits for a vegetated roof in such climate.

The impact of green roofs on the environment performance of buildings and cities remains an interesting subject of research. However, further investigations will be needed to assess if the green roof technology provides an efficient solution for building in energy savings, water management, acoustic, biodiversity, etc in cities under a tropical humid.

References

[1] Mentens J, Raes D, Hermy M. Green roofs as a tool for solving the rainwaterrunoff problem in the urbanized 21st century? Landsc Urban Plann 2006; **77**: 217 - 26.
[2] Fioretti R, Palla A, Lanza LG, Principi P. Green roof energy and water related performance in the Mediterranean climate. Build Environ 2010; **45**:1890 904.
[3] Yang J, Yu Q, Gong P. Quantifying air pollution removal by green roofs in Chicago. Atmos Environ 2008; **42**:7266 73.
[4] Li J-F, Wai OWH, Li YS, Zhan J-M, Ho YA, Li J, and al. Effect of green roof on ambient CO2 concentration. Build Environ 2010; **45**:2644 51.
[5] Van Renterghem T, Botteldooren D. In-situ measurements of sound propagating over extensive green roofs. Build Environ 2011; **46**:729 38.
[6] Schrader S, Böning M. Soil formation on green roofs and its contribution to urban biodiversity with emphasis on Collembolans. Pedobiologia 2006; **50**:347 56.
[7] Brenneisen S. Space for urban wildlife: designing green roofs as Habitats in Switzerland. Urban Habit 2006; **4**:27 36.
[8] Feng C, Meng Q, Zhang Y. Theoretical and experimental analysis of the energy balance of extensive green roofs. Energy Build 2010; **42**: 959 65.
[9] K. Liu, J. Minor, Performance evaluation of an extensive green roof, Presentation at Green Rooftops for Sustainable Communities, Washington DC, 2005.

[10] Castleton HF, Stovin V, Beck SBM, Davison JB. Green roofs; building energy savings and the potential for retrofit. Energy Build 2010; **42**:1582 91.
[11] Getter KL, Bradley Rowe D, Cregg BM. Solar radiation intensity influences extensive green roof plant communities. Urban Forest Urban Green 2009; **8**: 269 81.
[12] ROOFSOL, Building in ROOFSOL: Roof Solutions for natural cooling. In: Contract N° JOR3CT960074, Commission of the European Communities. DG XII, Science, Research and Development, 1998.
[13] Niachou A, Papakonstantinou K, Santamouris M, Tsangrassoulis A, Mihalakakou G. Analysis of the green roof thermal properties and investigation of its energy performance. Energy and Buildings, 2001; **33**, p.719-729.
[14] Spala A, Bagiorgas HS, Assimakopoulos MN, Kalavrouziotis J, Matthopoulos D, Mihalakakou G. On the green roof system. Selection, state of art and energy potential investigation of a system installed in an office building in Athens, Greece. Renewable Energy, 2008; **33**, p.173-177.
[15] Fioretti R, Palla A, Lanza LG, Principi P. Green roof energy and water performance in the Mediterranean climate. Building and Environment, 2010; **45**, p.1890-1904.
[16] Cappelli M, Cianfrini C, Corcicone M. Effects of vegetation roof on indoor temperatures. Heat Environ, 1998; **16**(2), p.85-90.
[17] Palomo E. Roof components models simplification via statistical linearization and model reduction techniques. Energy and Buildings, 1999; **29** (3), p.259-281.
[18] Good W. Factors in planted roof design. Constr. Specific, 1990; **43**(11), p.132.
[19] Wong NH, Cheong DKW, Yan H, Soh J, Ong CL, Sia A. The effect of rooftop gardens on energy consumption of a commercial building in Singapore. Energy and Buildings, 2003; **35**, p.353-64.
[20] Wong NH, Chen Y, Ong CL, Sia A. Investigation of thermal benefits of rooftop garden in the tropical environment. Building and Environment, 2003; **38**, p.261-70.
[21] Williams NSG, Rayner JP, Raynor KJ. Green roofs for a wide brown land: opportunities and barriers for rooftop greening in Australia. Urban Forest Urban Green 2010; **9** :245 51.
[22] Santamouris M, Pavlou C, Doukas P, Mihalakakou G, Synnefa A, Hatzibiros A, et al. Investigating and analysing the energy and environmental performance of an experimental green roof system installed in a nursery school building in Athens, Greece. Energy 2007; **32** :1781-8.
[23] Del Barrio EP. Analysis of the green roofs cooling potential in buildings. Energy Build 1998; **27**: 179 - 93.
[24] Sailor DJ. A green roof model for building energy simulation programs. Energy Build 2008; **40** : 1466 -78.
[25] Onmura S, Matsumoto M, Hokoi S. Study on evaporative cooling effect of roof lawn gardens. Energy Build 2001; **33**:653 - 66.
[26] Takakura T, Kitade S, Goto E. Cooling effect of greenery cover over a building. Energy Build 2000; **31**:1- 6.
[27] Djedjig R, Ouldboukhitine S-E, Belarbi R, Bozonnet E, Development and validation of a coupled heat and mass transfer model for green roofs, International communications in Heat and Mass Transfer, 2012; 39 752-761.
[28] S. Frankenstein, G. Koenig, FASST vegetation models, US Army Corps of Engineers® Engineer Research and Development Center, Technical Report TR-04-25, 2004, (available online : http://oai.dtic.mil/oai/oai?verb=getRecord&metadataPrefix=html&identifier=ADA428989).
[29] Alexandri E., Jones P., Developing a one-dimensional heat and mass transfer algorithm for describing the effect of green roofs on the built environment: comparison with experimental results, Building and Environment, 2007; **42** 2835–2849.
[30] He H., Jim C.Y, Simulation of thermodynamic transmission in green roof ecosystem, Ecological Modelling, 2010; **221** 2949–2958.
[31] Ouldboukhitine S-E, Belarbi R, Jaffal I,, Trabelsi A,, Assessment of green roof thermal behavior: a coupled heat and mass transfer model, Building and Environment, 2011; **46** 2624–2631.
[32] Tabares-Velasco P-C, Srebric J, A heat transfer model for assessment of plant based roofing systems in summer conditions, Building and Environment 2012 ; **49** 310–323.
[33] Ranaivoarisoa T.F. Modelisation dynamique monodimensionnelle des transferts hygrothermiques dans les toitures vegetalisees. M.Sc. report, University of La Réunion. 2012.
[34] Rakotondramiarana H.T. Etude théorique du séchage thermique et de la digestion anaérobie des boues des stations d'épuration-Mise au point des dispositifs pilotes de laboratoires pour la caractérisation expérimentale liée au séchage et à la méthanisation des boues. PhD Dissertation, University of Antananarivo. 2004. Available from: http://theses.recherches.gov.mg/pdfs/rakotondramiaranaherytiana_pc_doc3_04.pdf
[35] Rafieferantsoa M.H. Mise au point d'un code de calcul pour l'étude du comportement thermique des différentes composantes d'une toiture végétalisée, M.Sc. report, University of Antananarivo. 2011. Available from: http://theses.recherches.gov.mg/pdfs/rafieferantsoaMikaH_PH_M2_11.pdf
[36] Andriamamonjy A.L. Algorithme d'automatisation de la méthode d'analyse de sensibilité globale des modèles des systèmes complexes – application sur un modèle simulant une toiture végétalisée. M.Sc. report, University of Antananarivo, 2012. Available from: http://theses.recherches.gov.mg/pdfs/andriamamonjyAndoL_PC_M2_12.pdf
[37] Sébastien J. Performance énergétique d'une toiture végétale au centre-ville de Montréal. Summary of thesis. School of Higher Technology of Montreal. 2011. Available from: http://cremtl.qc.ca/fichiers cre/files/normandie/Performance_toiture_verte_2011.pdf (accessed on September 15th, 2012).